Physiological buffer effects in drug supersaturation - a mechanistic study of hydroxypropyl cellulose as precipitation inhibitor

Andreas Niederquell , Edmont Stoyanov , Martin Kuentz

PII: S0022-3549(23)00065-5
DOI: https://doi.org/10.1016/j.xphs.2023.02.013
Reference: XPHS 3020

To appear in: *Journal of Pharmaceutical Sciences*

Received date: 26 October 2022
Revised date: 14 February 2023
Accepted date: 14 February 2023

Please cite this article as: Andreas Niederquell , Edmont Stoyanov , Martin Kuentz , Physiological buffer effects in drug supersaturation - a mechanistic study of hydroxypropyl cellulose as precipitation inhibitor, *Journal of Pharmaceutical Sciences* (2023), doi: https://doi.org/10.1016/j.xphs.2023.02.013

Physiological buffer effects in drug supersaturation - a mechanistic study of hydroxypropyl cellulose as precipitation inhibitor

Andreas Niederquell[1], Edmont Stoyanov[2], Martin Kuentz[1]

[1]*School of Life Sciences*, *University of Applied Sciences and Arts Northwestern Switzerland, CH 4132 Muttenz, Switzerland*

[2]*Nisso Chemical, Europe, Berliner Allee 42, 40212, Düsseldorf, Germany.*

Graphical abstract

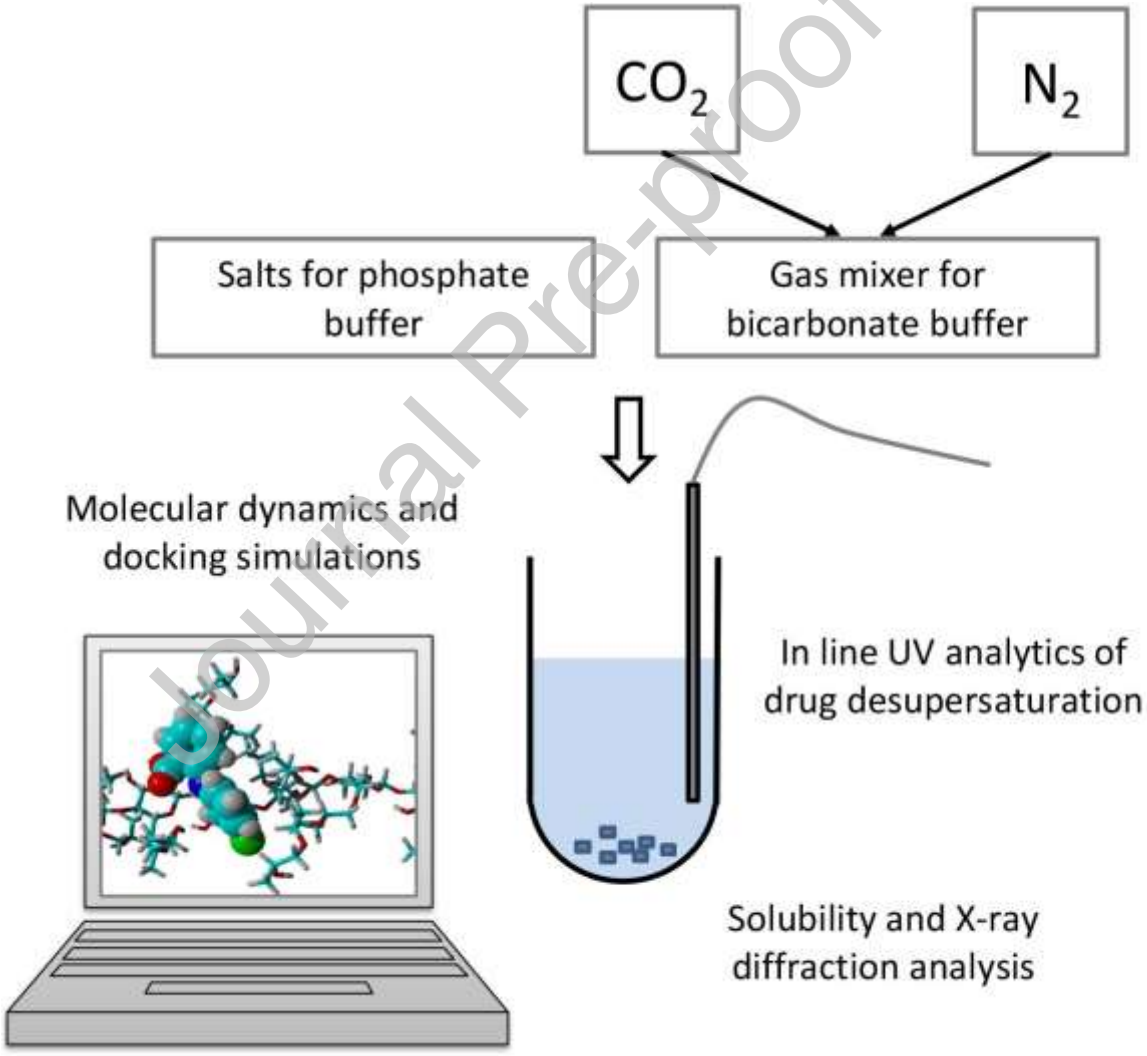

ABSTRACT

Phosphate buffer is predominantly used instead of the more physiological bicarbonate buffer, as the latter requires a technical solution of adequate gas mixing. Recent pioneering work on how bicarbonate buffer affected drug supersaturation revealed interesting effects that call for more mechanistic understanding. Therefore, this study used hydroxypropyl cellulose as a model precipitation inhibitor and real-time desupersaturation testing was conducted with the drugs bifonazole, ezetimibe, tolfenamic acid and triclabendazole. Specific buffer effects for the different compounds were noted and overall, statistical significance was found for the precipitation induction time (p = 0.0088). Interestingly, molecular dynamics simulation revealed a conformational effect of the polymer in the presence of the different buffer types. Subsequent molecular docking trials suggested a stronger interaction energy of drug and polymer in the presence of phosphate compared to bicarbonate buffer (p =0.0010). In conclusion, a better mechanistic understanding of how different buffers affect drug-polymer interactions regarding drug supersaturation was achieved. Further mechanisms may account for the overall buffer effects and additional research on drug supersaturation is certainly needed, but it can already be concluded that bicarbonate buffering should be used more often for *in vitro* testing in drug development.

Keywords: Formulation, solubilization, supersaturation, precipitation, molecular modeling

Introduction

Phosphate buffers are predominantly used for *in vitro* testing, including drug release and supersaturation studies, even though the intestine is known to have a bicarbonate- CO_2 buffering system.[1] The main reason for *in vitro* tests with a less physiological buffer is technical simplicity, as opposed to a bicarbonate buffer system where dissolved CO_2 has the

tendency to volatize. Therefore, a technical approach is to continuously sparge the solution with CO_2 gas or alternatively with inert N_2 gas (for lowering CO_2 in solution) to achieve an equilibrated physiological buffering system at the targeted intestinal pH. Technical solutions for such physiological buffering systems are now available, from individual pH adjustment to simulation of entire pH profiles along the gastro-intestinal (GI) tract. [2-5] An alternative to replacing the lost CO_2 in solution is to prevent gas evaporation from bicarbonate buffer solutions by the recently introduced floating lid method.[6] While this method has the advantage of simplicity, there are also limitations, for example, if a pH change is simulated during *in vitro* experiments. However, these different technical developments in the field of bicarbonate buffering underline the current interest in this biopharmaceutical topic.

An important finding of physiological buffering research was that drug release from coated dosage forms was significantly affected by whether a bicarbonate or phosphate buffer was selected[7] and the relevant *in vivo* release data was indeed in favor of using a bicarbonate buffer (Varum et al., 2014).[8,9] The effects of physiological buffering were not only demonstrated with polymer-containing formulations but intrinsic dissolution kinetics of different ionizable drugs were also shown to depend on the choice of the buffer species. [10-12] An interesting peculiarity was the hydration-dehydration kinetics of the bicarbonate-CO_2 system. It is typically assumed that ionization reactions are nearly instantaneous compared to drug diffusion across the boundary layer. However, the hydration-dehydration kinetics appears to be comparatively slow in the fluid boundary layer, leading to an apparently effective pK_a that controls dissolution of ionizable compounds.[13] The latter work is a good example of the recent advances in studying physiological buffering although much is still unknown, both on the level of pharmaceutical applications as well as mechanistic understanding.

Recent pioneering work investigated bicarbonate buffering in the field of drug supersaturation and precipitation using poorly soluble drug bases.[14] The latter compounds

often show a natural supersaturation upon transfer from acidic stomach medium to intestinal fluids, where the higher pH leads to decreased solubility.[15,16] The pioneering study simulated this transfer *in vitro* and used hydroxypropyl methylcellulose acetate succinate (HPMCAS) as drug precipitation inhibitor (PI), as such polymers are widely used in supersaturating formulations to sustain high luminal drug levels.[17-19]. A delayed and reduced precipitation upon addition of HPMCAS was indeed observed in the case of the tested drug bases (i.e., ketoconazole, pazopanib and lapatinib) using phosphate buffer. Interestingly, there was no longer such a marked polymer effect on drug precipitation with the same experimental conditions, but using bicarbonate as buffer in the simulated intestinal medium, which agreed with an *in vivo* rat study that showed no significant advantages regarding drug exposure upon addition of HPMCAS.[14] A follow-up study of this collaboration between the University of Greifswald and Merck KGA in Germany provided data from further *in vitro* transfer pH-shift experiments using ketoconazole, cinnarizine, amiodarone HCl and dipyridamole.[20] As a result, there was no marked effect of the buffer type noted on the observed concentration profiles. However, there was no PI used in these latest experiments, so it appears that pronounced buffer effects in transfer experiments may occur on the level of drug-polymer interactions. This recent seminal study also tested solubility and dissolution of 26 compounds of which the majority showed statistically significant differences in their kinetic dissolution parameters, while only some compounds revealed a statistical effect of the buffer system on thermodynamic solubility.[20]

The authors discussed a series of possible mechanisms to explain the buffer effect including common ion effects, solubility of salts, surface pH and buffer influences on drug wettability. It is here important to mention that these recent experiments used fasted state simulated intestinal fluid (FaSSIF)[21-23] and hence colloids consisting of bile salt and phospholipids were present, which is in general more bio-relevant than simple buffer media, but it certainly adds a level of complexity to the mechanistic discussion of buffer effects.

To better understand the mechanisms underlying observed buffer effects, further research is needed. The present study aims to provide a better understanding of bicarbonate vs. phosphate buffer effects on drug-polymer interactions for supersaturating drug formulations. Hydroxypropyl cellulose was used as a model polymer based on a recent interest in this excipient for supersaturating drug delivery systems.[24-27] A particular aim of the present research was to use molecular dynamics (MD) simulations and molecular docking to investigate how buffer ions interact with a given drug-polymer system in bulk solution. Modeling of entire crystals was beyond the scope of the present MD simulations, but the relative extent of drug-excipient interactions in bulk solution can also matter for the corresponding interfacial drug-excipient interactions.

For experimental comparison, solvent-shift experiments with in-line UV spectroscopy are being conducted to study desupersaturation kinetics of the model drugs bifonazole, ezetimibe, tolfenamic acid, and triclabendazole. Finally, we aim to obtain new mechanistic insights into how physiological bicarbonate buffering affects supersaturated drug in the presence of a cellulosic precipitation inhibitor.

Materials and methods

Materials

The chemicals sodium chloride, sodium phosphate monobasic and ethanol were obtained from Sigma Aldrich (Schaffhausen, Switzerland); sodium bicarbonate was purchased from Honeywell Fluka (Schaffhausen, Switzerland). As for the precipitation inhibitor, HPC of grade L (molecular weight of around 134 000 g/mol with ~75% (w/w) content of hydroxypropyl groups)[27] was kindly donated by Nippon Soda Co., Ltd. (Tokyo, Japan).

The active compounds were selected arbitrarily as model for poorly soluble drugs. Bifonazole, tolfenamic acid and triclabendazole were purchased from Carbosynth Ltd. (Compton, UK), while ezetimibe was obtained from Molekula Ltd. (Darlington, UK). All materials were used as received.

Methods

Solubility assay and residual solid-state analysis by X-ray powder diffraction

Buffers were prepared in line with the relevant pharmaceutical literature and the composition[14] can be inferred from Table 1. For thermodynamic solubility measurements, the different drugs were added to the two aqueous buffer solutions in excess and magnetically stirred (800 rpm) for 48 h at 37°C. Subsequently, the residual solid was separated from the aqueous phase by vacuum filtration and the supernatant was passed through a syringe filter (0.45 µm, PTFE Titan 3 filters, 17 mm). The drug concentrations were measured at 37°C in triplicate using the same UV equipment used for the kinetic desupersaturation experiments, i.e., a model 440 UV−vis spectrophotometer from SI Photonics Inc. (Tucson, USA) with a UV fiber optic dip probe (1 cm path length). For each drug, entire spectra from 200 – 450 nm were recorded and 20 datapoints were collected at the different drug-specific absorption maxima (i.e., bifonazole 258 nm, ezetimibe 232 nm, tolfenamic acid 283 nm, triclabendazole 304 nm) to obtain a single solubility estimate, which was repeated in triplicate.

For the carbonate buffer, the equilibration samples were stirred magnetically in a water bath at 37°C (800 rpm) using vials in which the closed lid of the glass vial contained a hose that was directly connected to the supply of CO_2 and N_2 of the gas mixing unit KM 10-2 FLEX by WITT-Gasetechnik GmbH & Co KG (Witten Germany). Gas supply was regulated to keep pH constant at 6.5, which was regularly checked throughout the experiment. Following the

48 h equilibration time, samples were prepared for subsequent UV analysis as described above.

Regarding solid-state analysis of the different drugs, the residual solid was collected from the vacuum filtration described and subjected to additional drying in a vacuum oven (60°C for 24 h and 100 mbar vacuum). These samples were then analyzed by X-ray powder diffraction (XRPD) analysis and compared to untreated neat drug. The analytical X-ray diffraction patterns were obtained using an X-ray diffractometer (D2 Phaser) from Bruker AXS Ltd. (Karlsruhe, Germany) equipped with a Cu KFL tube (30 kV, 10 mA) as the radiation source and a Lynxeye® detector. Each sample was automatically rotated on a sample holder at 15 rpm, and the angular scanning range for each sample was from 6° (2θ) to 42° (2θ) with a 0.016° step size (2θ) at 2.0 s per step.

Kinetic desupersaturation assay by in-line UV spectroscopy

The kinetic assay of drug desupersaturation also used the buffer media as described in the literature and summarized in Table 1.[14] For the bicarbonate buffer, a gas mixing unit type KM 10-2 FLEX by WITT-Gasetechnik GmbH & Co KG (Witten Germany) was used to dynamically add either N_2 or CO_2 gas to keep the pH constant at 6.5. Apart from pure buffer solutions, phosphate and bicarbonate buffer solutions were prepared that included 0.01% (w/w) of HPC (grade L) from Nippon Soda Co., Ltd (Tokyo, Japan). The freshly prepared polymer-containing solutions were left for 24 h (room temperature with 500 rpm magnetic stirring) of equilibration prior to use. Thus, to prepare for kinetic desupersaturation experiments, the solutions were warmed to 37°C using magnetic stirring at 200 rpm for one hour. Concentration analysis was based on a model 440 UV−vis spectrophotometer from SI Photonics Inc. (Tucson, USA), which was equipped with a UV fiber optic dip probe (1 cm path length). Following measurements of the pure buffer or polymer-containing buffer solutions, methanolic drug solutions with individual concentrations were added as 2.2 ml

methanol solution to 217.8 ml of the different aqueous buffer solutions to yield a final volume of 220 ml. Subsequently, UV absorbance was recorded for drug-specific wavelengths (as described previously for solubility determination) every 0.5 minutes (or in some cases every minute) for a total duration of 2 h. To mark the onset of precipitation (or induction time), the time was taken for which the absorbance vs. time curve showed an initial -5% change in absorbance relative to the initial plateau concentrations. Absence of such a plateau suggests an induction time of zero, whereas for samples with a best excipient effect (i.e., parachute effect)[28], the maximum experiment duration was taken as induction time. This was a pragmatic approach and further in line with the idea that differentiation of induction times that go beyond the intestinal transit time would not be of biopharmaceutical relevance.[29] The initial (maximum) drug concentrations in this desupersaturation assay were 20 µg/ml for bifonazole , 80 µg/ml for ezetimibe, 100 µg/ml for tolfenamic acid and 30 µg/ml for triclabendazole.

Molecular modeling

The software MarvinSketch v.19.3 (ChemAxon Ltd, Budapest, Hungary) was used to calculate distribution coefficients at pH 6.5, $logD_{6.5}$ and pK_a values of the different model drugs.

MD simulations and docking trials were enabled by the YASARA software v. 20.12.24 (YASARA Biosciences GmbH, Vienna, Austria).[30] Automated pKa prediction was used to determine the protonation state of major microspecies at pH 6.5[31] and acceleration was by graphics processing units (GPUs) for calculation of the non-bonded interactions (Van der Waals and real-space Coulomb forces).[32] A GLYCAM force field [33]of the AMBER 12 family was used for the HPC model. This polymeric model had 40 monomers (n=40) for the MD simulations to calculate solvent accessible surface area (SASA) (simulation cell of 180x 90x 90 Å), while a smaller HPC oligomer of n= 20 was selected for other MD simulations to

prepare for molecular docking (120x 60x 60 Å simulation cell). These HPC models were based on ^{13}C-nuclear magnetic resonance (NMR) spectra to reflect the polymer's degree of substitution as well as the molar substitution combined. As for the drug models, a general AMBER force field, GAFF2[34] was employed, wherein atomic charges were based on a semi-empirical quantum chemical estimation (AM1BCC).[35] Thus, so-called RESP-like charges were obtained, which means that through the use of a restraint function during the fitting of the potential charges to electrostatic potentials, the magnitude of the charges may be attenuated (i.e., restrained electrostatic potential charges).

Finally, water molecules were explicitly taken into account by the widely used TIP3P model[36] wherein dissolved ions were selected to reflect a corresponding bulk concentration in the simulation cell in line with Table 1. Periodic boundary conditions were selected and following steepest decent and simulated annealing minimizations to remove clashes, the simulations were run for 5 ns. Equations of motion were integrated with a 2x 1fs timestep as an NTP ensemble with a temperature of 310 K, where the pressure control was achieved by rescaling the simulation cell along the x,y, and z axis to reach a constant pressure of 1 bar. A cutoff value of 8 Å was selected for the Van der Waals forces and the particle mesh Ewald algorithm was applied to electrostatic forces.[37] The MD simulations were run in triplicate by varying the initial placement of the molecules in the simulation box.

To study the polymeric interactions with the different drugs *in silico*, an n=20 HPC model was prepared by an MD simulation according to the protocol described above and was then used in a second step for molecular docking. The AutoDock VINA software[38] was employed for automated docking within the YASARA modeling platform by using default parameters. AutoDock VINA is a commonly used computational approach to search the conformational space of how ligands bind to polymers. Within YASARA the aforementioned quantum-chemical calculations (AM1BCC) are used to obtain RESP-like partial charges, which are then further tuned for maximum compatibility with the Autodock scoring function. 25 automated runs were conducted, and results were clustered according to binding modes.

From the latter runs differing in their binding modes, an average interaction energy of drug and HPC was calculated where negative values indicate high drug binding to polymer.

Statistical analysis

Statistical analysis was based on the software program Statgraphics Centurion 18th Professional edition (v. 18.1.06) from Statgraphics Technologies Inc. (Warrenton, USA). For comparison of the induction times of the kinetic experiments with added 0.01% (w/w) HPC, a one-factor Kruskal-Wallis test was conducted to cope with unequal variances. Analysis of the variance (ANOVA) was conducted for comparing the different solubility values as well as molecular simulation runs. In general, *p*-values were reported to express the probability of a true null hypothesis (whereby $p < 0.05$ suggests significance of an effect). Post-hoc comparison between groups used Tukey's honestly significant difference (HSD) at the 95% significance level.

Results and discussion

Drug solubility in buffers and residual solid analysis

As initial characterization, drug solubility was measured in the different buffers and residual solid was analyzed by XRPD to identity possible solvent-induced phase transformations. The solubility results are outlined in Table 2 and a two-way ANOVA of drug and buffer-type revealed that both factors and their interaction were highly significant with $p < 0.0001$ in each case. Bifonazole was special in that it was the only drug for which the solubility in phosphate buffer was higher than in the physiological buffer, whereas the opposite was the case for the solubility of ezetimibe, tolfenamic acid and triclabendazole. In relative terms, the higher solubility in bicarbonate buffer was most pronounced for triclabendazole, but in terms of absolute difference tolfenamic acid was also noteworthy. This can be compared to the recent

work of Krollik et al.[20] in which only some of the investigated drugs showed statistically significant differences in solubility by comparing phosphate vs. bicarbonate buffer. However, the latter work used the buffers as part of FaSSIF, so the situation is different in that bile salts and phospholipids were present. The colloids in FaSSIF would solubilize especially drugs that are poorly water-soluble,[39] which may attenuate relative differences between buffer species. Noteworthy is further that FaSSIF contained a lower phosphate concentration than in the present study or that of Jede et al.[14], which may have further contributed to a comparatively lower buffer effect on solubility.

As for the residual solid-state analysis in the current study, the drugs tested showed nearly the same XRPD pattern of the neat drug and the dried excess drug that was collected from the solubility studies in the respective buffer systems at pH 6.5 (Fig. 1). The most characteristic Bragg peaks corresponded well to previously published articles on bifonazole[40] and ezetimibe anhydrate.[41] As for tolfenamic acid, the diffractogram compares adequately with form I.[42] Finally, the diffraction pattern of triclabendazole again appeared to fit best with the known solid form I.[43] Fig. 1 displays nearly superimposable diffractograms of neat drug and compound obtained for all model drugs as residual solid from the solubility tests in the respective buffer systems. Therefore, no indication was given that a solvent-mediated phase transformation occurred, which otherwise would have the potential to affect drug concentrations *in vitro* and/or *in vivo.* Although it is theoretically possible that experimental sample preparation with a drying step could miss a transient metastable solid formed in aqueous medium, this was not a likely mechanism to account for differences observed between the buffers.

Desupersaturation studies using in-line UV analytics

A solvent-shift assay in in-line UV analytics was used to study desupersaturation behavior of the different model drugs in the presence of HPC. Such assays have merits especially in the

early phase of drug formulation development to select a bio-enabling formulation principle and suitable excipients for drug precipitation inhibition.[16,18,44] Fig.s 2 and 3 show the concentration profiles of the selected model drugs obtained for a maximum of two hours. Individual profiles are given to provide more detailed information on the precipitation events as opposed to relying on mean values only. Fig. 2A shows experiments of the weakly basic drug bifonazole (pK_a= 6.4; $logD_{6.5}$= 5.1) in phosphate buffer, whereas Fig. 2B presents the corresponding kinetics with physiological buffering using bicarbonate. In absence of polymer, drug precipitation started immediately, while addition of 0.01 % (w/w) HPC (L-grade) showed a clear precipitation inhibition effect, which has been previously called a parachute effect.[28] Interestingly, this polymer- effect was not more pronounced in phosphate buffer, which was shown previously with ketoconazole, pazopanib-HCl, and lapatinib-ditosylate.[14] Even though these compounds are also weakly basic drugs, their supersaturation in this previous study was induced by a pH-shift experiment and the precipitation inhibitor was 0.1% (w/w) hydroxypropyl methylcellulose acetate succinate (HPMCAS), which points to the importance of gathering additional experimental results before more general conclusions can be drawn. Fig. 2C shows the concentration profiles of the apparently neutral compound ezetimibe ($logD_{6.5}$= 4.6) and here the added 0.01 % (w/w) HPC greatly sustained drug supersaturation compared to pure drug in phosphate buffer. This can be compared with a previous solvent-shift supersaturation study of ezetimibe in which 0.05 and 0.1 % (w/v) polyvinylpyrrolidone (i.e., PVP K30) were added to FaSSIF with phosphate buffer whereby a marked effect of polymer on drug precipitation was also shown.[45] However, the present study also investigated ezetimibe in bicarbonate buffer (Fig. 2D) in which some parachute effect was observed, but the onset of precipitation already occurred after only a few minutes with a more gradual decline of concentrations. Thus, these results are comparable to the findings in the pioneering study of Jede et al[14] (who used a transfer pH-shift experiment), in that a greater parachute effect was evidenced in phosphate buffer compared to the more physiological bicarbonate buffer.

Unlike the other model compounds, tolfenamic acid has an acidic pK_a of 3.9 ($logD_{6.5}$= 3.0) and Fig.s 3A and B show that some delay in precipitation is also seen for pure drug. Although phosphate buffer (Fig. 3A) displayed earlier drug precipitation than in bicarbonate buffer (Fig. 3B), the difference was not substantial from a biopharmaceutical perspective. This was different in the case of the added 0.01% (w/w) HPC, which showed clear differences between the buffers. In phosphate buffer, maintained supersaturation was noted throughout the experiment, whereas in bicarbonate buffer, tolfenamic acid showed first precipitation after about half an hour. The view of a more pronounced buffer effect in the presence of even low amounts of polymer is interesting and would agree with recent work that studied differences in FaSSIF with either phosphate or bicarbonate buffer regarding solubility or a pH-shift transfer test but without addition of any polymer. Depending on the compound used, either no effect or moderate effect of the buffers was noted.[20] There is of course the aforementioned possibility that colloids in FaSSIF may attenuate buffer differences. However, in terms of kinetic experiments in the pH-shift assay of the Jede et al. study,[14] the addition of 0.1 % (w/v) HPMCAS displayed marked differences in precipitation between the two buffers even though FaSSIF was used. This supports the view mentioned in the introduction that specific ions in the buffer can play an important role in how a drug interacts with polymer.

As for the specific case of tolfenamic acid, previous work studied a potential relationship between glass forming ability[46,47] and supersaturation propensity.[48,49] This previous work showed that good glass formers also seem to exhibit potential to supersaturate to a high degree, whereas modest glass formers may supersaturate only to a lesser degree. However, with respect to the onset time of precipitation, the authors could not find a correlation.[48] As the *in vitro* tests used amorphous drug, the poor glass formers such as tolfenamic acid were excluded from the study. It is interesting to note that poor glass-forming drugs are often

carboxylic acids and they have potential to self-interact as acid dimers, as has been shown for tolfenamic acid in ethanol solution for drug crystallization.[50] While much is still unclear about how such interactions in solution phase translate into crystal nuclei and growth of crystals, it seems that carboxylic acids represent a special case owing to their ability to self-interact.

As a further model compound, triclabendazole with a basic pK_a of 4.4 and an acidic pK_a of 10.3 ($logD_{6.5}$= 5.9) was selected. Fig. 3C displays the desupersaturation kinetics in phosphate buffer where pure drug started to precipitate again right from the start of the experiment but 0.01% (w/w) HPC continuously sustained the metastable supersaturated concentrations during the entire experiment duration of 120 min. The physiological buffer by comparison (Fig. 3D) also showed an immediate onset of precipitation for pure drug as well as some parachute effect of HPC, but initial precipitation was already observed after about a quarter of an hour, when desupersaturation continued slowly but steadily.

In summary, the determined induction times from the different kinetic curves can be inferred from Table 3. A clear parachute effect of 0.01% HPC addition was evident in line with the previous discussion of the kinetic profiles. It was interesting whether the samples with added polymer would show a buffer effect and the *p*-value here was 0.0088, which confirms the significant influence of the buffer choice.

Molecular dynamics simulations of HPC in phosphate buffer vs. bicarbonate

It is crucial to achieve a better understanding of the buffer effect in the field of drug supersaturation. Buffer ions can in principle play a role both in bulk solution and on the surface of drug nuclei/crystals to affect the overall process of drug precipitation. While the mechanisms of drug precipitation are in general well researched,[51] how these mechanisms are influenced by buffer ions is not well known. This paper focuses on the mechanisms

occurring in bulk solution to better understand the excipient's parachute effect even though there can be also relevance of the conducted molecular simulations for drug-polymer interactions on the surface of precipitated drug nuclei. We used a molecular model of HPC that has been developed based on ^{13}C-nuclear magnetic resonance (NMR) spectra. This is important because different HPC qualities that comply with compendial specifications can still vary on a molecular level. Thus, degree of substation (DS) or molar substation combined (MS) can show differences and even for grades with a similar viscosity, the molecular weight (MW) distribution can vary between suppliers.[52] A first set of MD simulations was conducted in absence of drug to study *in silico* how the buffer ions would affect HPC. This was a first step followed by molecular docking to investigate how possible conformational changes would affect drug-polymer interactions in solution.

As for the drug-free polymer solution, Fig. 4A shows a snapshot of an MD simulation after 5 ns in phosphate buffer and Fig. 4B, the corresponding result in bicarbonate buffer by targeting a model of buffer concentrations given in Table 1. The ions are given in the ball-and-stick model for better visualization while HPC is depicted as tube model with the solvent accessible surface area (SASA). The *in silico* results suggested that neither the dihydrogen phosphate nor the bicarbonate ions were showing a marked accumulation on the polymer surface. This is interesting to compare with recent insights into Hofmeister ion effects, suggesting surface accumulation or exclusion on biopolymers or hydrocarbons was highly specific for given ions.[53] While weakly hydrated ions with large polarizability tend to interact directly with a polymer surface, whereas the strongly hydrated ions with smaller polarizability would rather interact from the bulk phase via the hydration shell.[54] This view and the specific analysis of surface ion accumulation/exclusion is useful, but some care is needed when using the classical distinction of so-called "chaotropic" vs. "kosmotropic" ions. Despite recent theoretical advancements, there are still theoretical gaps and more about this theoretical discussion of Hofmeister ion effects can be inferred from the literature.[54-56]

The lack of any clear surface accumulation of ions in the present MD simulations agrees with the view that both the dihydrogen phosphate and bicarbonate ions are strongly hydrated, so the polymer HPC would be rather indirectly affected via the hydration layers. As these ions are of a similar type, an important question was whether a distinction could be made with respect to the conformational structure of HPC. Therefore, the SASA was calculated, and the 5 ns reference time was compared to the initial value in Table 4. Both types of buffers led to a loss of SASA but the value was more pronounced in the case of phosphate buffer. Statistical analysis showed that SASA changes over time were highly significant and the differences between buffers were found to be significant too. Comparing the size of the model HPC in the MD simulations with a MW of ~13kD with the experimentally used L-grade of MW ~ 140 kD, the considerably larger real polymer has more possibilities to undergo conformational changes in presence of buffer ions. Another recently mentioned point is that aggregation of HPC chains can lead to further solubilizing domains for drugs and hence more complexity.[27] Thus, although the *in silico* obtained differences in SASA were of a comparatively small extent between the buffers, it can be expected that the much larger real HPC may undergo more pronounced conformational differences with a possible aggregation of polymer chains.

Another aspect of the experimental situation is that the bicarbonate buffer comes with some dissolved and dispersed gas, which certainly adds another layer of complexity to studying ion effects mechanistically.[55] Dissolved gas or even small gas bubbles could only be considered *in silico* by using much larger scale MD simulations. Bearing in mind that drug nucleation on the air-interface is a separate possible mechanism of experimental desupersaturation, it was remarkable that already the presented molecular simulations of the aqueous bulk with given limitations of scale and duration were able to identify conformational polymer changes caused by the different buffers. A next research question in the present work was then whether such changes would be relevant for the molecular interactions of drug and polymer.

Molecular docking simulations of drug and HPC in the different buffers

Based on the differences obtained in SASA of HPC in the presence of the different buffers, it was then interesting to study a possible influence of how the polymer would interact with the different drugs. Molecular docking was conducted on HPC oligomers (n=20) that were prepared *in silico* in the two buffer systems by MD simulations with the same protocol as in the *in silico* trials to calculate the SASA. The subsequent docking computer experiments yielded valuable insights into how the drugs most probably interacted with HPC. The average energies are displayed in Fig. 5 and bifonazole tended to interact more strongly with HPC in phosphate buffer compared to bicarbonate buffer even though the 95% Tukey intervals still showed some overlap.

Fig. 6 and Fig. 7 show, for each drug and buffer system, the conformation with the most negative interaction energy. In case of bifonazole (Fig. 6 A and B), HPC appeared to embrace the compound with side arms to minimize the contact of hydrophobic groups with water. This was especially relevant in the case of the aromatic rings and can be compared to a previous study of how drugs interacted with Eudragit EPO.[57] This previous work used ^{1}H NMR spectroscopy and suggested that the aromatic drug moieties especially were involved in the interaction with polymer. This is similar to the present study, in which the HPC side arm can interact via Van der Waals interactions or via Lewis acidity of hydroxyl groups with the aromatic electron cloud of a drug. A comparison of the buffers in Fig. 6A and B should be interpreted with care as only the most stable conformation is shown and obtained interaction energies were calculated for the average of all binding conformations obtained from molecular docking.

Fig. 6C and D depict the lowest energy conformations for the HPC-drug interaction with ezetimibe. This drug had the highest energy difference between buffers with the stronger molecular interaction in the case of phosphate buffer. This can be compared to the kinetic experiments, in which a more pronounced parachute effect with longer induction time was found for ezetimibe in this buffer (Table 3). This also compares well with the pioneering study of Jede et al.[14] in which pH- shift experiments of three drug bases and 0.1% HPMCAS showed a stronger parachute effect in phosphate compared to bicarbonate buffer. Thus, some care is needed if precipitation experiments only run in conventional phosphate buffer because the extent of an excipient effect on drug supersaturation can apparently be different in the physiological buffer.

As in the previous drug case, according to our molecular docking results ezetimibe interacted with the polymeric side arms (Fig. 6 C and D). Such polymeric “nesting” was probably affected by the surrounding ions, which agrees with the previous MD simulation results suggesting a smaller SASA in presence of phosphate vs. bicarbonate ions, thereby leading to comparatively better shielding of a hydrophobic drug from the aqueous environment. However, such a molecular mechanism would play a role especially in the case of dominant hydrophobic drug interaction; in other cases in which hydrogen bonding is observed between drug and polymer the situation can be different again.

The most stable conformations of HPC and tolfenamic acid are shown in Fig. 7A and B for phosphate and bicarbonate buffer respectively. As a result, to some extent there were also interactions with side arm leading to the drug being nested in HPC, not unlike the other compounds used in this study. This is interesting to compare with a recent MD simulation of celecoxib and HPC for which 0.1 N HCl and phosphate buffer pH 6.8 were compared.[27] In the MD simulation the drug was somewhat exposed to the aqueous phase and hydrogen bonding was only observed at pH 6.8.[27] This previously work did not consider physiological buffering, but for higher polymer concentrations it showed that a non-linear increase in drug solubilization occurred. Accordingly, the molecular view from individual polymer chains

interacting with drug primarily reflects the situation at high dilution. For higher polymer concentrations, a drug may find further opportunities to interact, for example, between overlapping chains, so the current molecular simulations should be viewed as a first approximation of what happens in bulk solution.

Tolfenamic acid was the only compound in the present molecular docking study for which practically no difference was observed between the two buffers, as can be inferred from Fig. 5. However, a longer induction time was again observed at 0.01% HPC compared to the corresponding experiments using bicarbonate buffer (Table 3). Although the bulk interaction of drug and polymer is expected to be of key importance, there are still additional effects that play a role in case of the solvent-shift experiments. Drug growth inhibition on the surface of crystal nuclei is one of such additional effects and it was mentioned before that tolfenamic acid tends to self-interact in solution.[50] In principle, all these molecular mechanisms could be influenced by buffer species, and the lack of an overall experimental effect could mean that either different molecular mechanisms canceled each other out or there was simply not much of an ion-mediated effect in this case.

As for triclabendazole, the interaction with HPC is shown in Fig. 7 C for phosphate buffer and in Fig. 7 D for bicarbonate, whereby the most stable conformation is shown in line with how the docking results were presented with the other drugs. There is a longest axis in this molecule and interestingly, this axis was quite differently oriented depending on the buffer. However, in both buffer types, the compound was rather nested in the polymer based on side-arm interactions. This is comparable with the previously discussed drugs for which hydrophobic moieties were shielded from the aqueous environment. A further similarity to other compounds was that the average interaction energy was stronger in phosphate buffer compared to that in bicarbonate buffer (Fig. 5). This also fits well with the view that a pronounced precipitation inhibition was observed in phosphate buffer, whereas again a relatively lower parachute effect was noted for bicarbonate buffering (Table 3).

Statistical valuation of all docking results showed in a two-factor ANOVA that interaction energy with HPC was drug specific ($p < 0.0001$) and an overall effect of the buffer species was observed ($p = 0.001$). Moreover, the interaction between these two factors was found to be significant ($p = 0.0164$) so the buffer effect clearly depended on the given drug, as displayed in Fig. 5.

Regarding the overall drug-HPC interactions studied in the current work, it was interesting to note that with all compounds there was some degree of side-arm interactions, leading to some polymeric drug nesting. This leads to many contact points for Van der Waals interactions between drug and polymer, so their net effect can be dominant even though on individual contact points they are weaker than polar interactions or hydrogen bonding. Another point that can be summarized based on the observed polymer nesting is that the side arm structure appears to be particularly relevant for excipient performance. It was mentioned earlier that the present computer models simulated the given HPC polymer based on structural knowledge of DS and MS values.[27] There can be differences in these side arm structures for different HPC qualities, and this should be kept in mind when excipients of different suppliers are compared. It seems that such details can matter, at least when using cellulose derivatives such as HPC for precipitation inhibition of poorly water-soluble drugs.

Conclusions

Physiological buffering has gained much attention with the availability of modern technical possibilities to keep pH either constant or to alter it in a computer-programmed manner to simulate *in vitro* the changes in gastro-intestinal transit. Results of recent pioneering work on buffer effects in drug supersaturation sparked particular interest, but also led to some open

mechanistic questions. Therefore, the present research aimed to gain mechanistic insights by using full-atomistic MD simulations and it was an interesting finding that the SASA of the model polymer HPC was found to be dependent on the buffer selected. Although these were comparatively subtle changes, they translated to differences in molecular docking of drug and HPC. This points to the relevance of polymer conformation and topology to enable specific molecular interactions with the drug. Moreover, it is noteworthy that the extent of the buffer effect in molecular docking depended significantly on the drug given. Experimentally, a statistically significant buffer effect was also observed in the solvent-shift desupersaturation assay. The latter test involves not only drug-polymer interactions in the aqueous bulk phase, but HPC may also adsorb to crystal surfaces as a separate mechanism to reduce precipitation by hindering particle growth. Thus, precipitation inhibition is a complex process based on more than one mechanism so modeling of bulk interactions may provide an incomplete representation of what happens in solubility or desupersaturation experiments but the present paper sheds light on how the drug-polymer interactions in the bulk phase can be affected by buffer species. This improved physico-chemical understanding is not only relevant for making sense of *in vitro* data but would further help to target more predictive correlations with *in vivo* results, which would also concern physiologically based pharmacokinetic modeling. There is surely more research to be done in the future but already today it can be concluded that physiological buffering should be increasingly used for *in vitro* testing, especially regarding evaluation of any drug-polymer interactions.

Declaration of interests

The authors declare the following financial interests/personal relationships which may be considered as potential competing interests: Edmont Stoyanov is an employee of Nisso Chemical Europe GmbH.

Acknowledgments

The authors wish to thank Nisso Chemical Europe GmbH for funding this research project. Research data used in preparation of the manuscript can be obtained from the corresponding author upon request.

REFERENCES

1. Hens B, Tsume Y, Bermejo M, Paixao P, Koenigsknecht MJ, Baker JR, Hasler WL, Lionberger R, Fan JH, Dickens J, Shedden K, Wen B, Wysocki J, Loebenberg R, Lee A, Frances A, Amidon G, Yu A, Benninghoff G, Salehi N, Talattof A, Sun DX, Amidon GL 2017. Low Buffer Capacity and Alternating Motility along the Human Gastrointestinal Tract: Implications for in Vivo Dissolution and Absorption of Ionizable Drugs. Molecular Pharmaceutics 14(12):4281-4294.
2. Garbacz G, Kolodziej B, Koziolek M, Weitschies W, Klein S 2014. A dynamic system for the simulation of fasting luminal pH-gradients using hydrogen carbonate buffers for dissolution testing of ionisable compounds. European Journal of Pharmaceutical Sciences 51:224-231.
3. Garbacz G, Rappen GM, Koziolek M, Weitschies W 2015. Dissolution of mesalazine modified release tablets under standard and bio-relevant test conditions. Journal of Pharmacy and Pharmacology 67(2):199-208.
4. Silva DA, Al-Gousous J, Davies NM, Chacra NB, Webster GK, Lipka E, Amidon G, Lobenber R 2019. Simulated, biorelevant, clinically relevant or physiologically relevant dissolution media: The hidden role of bicarbonate buffer. European Journal of Pharmaceutics and Biopharmaceutics 142:8-19.
5. Wulff R, Rappen GM, Koziolek M, Garbacz G, Leopold CS 2015. Controlled release of acidic drugs in compendial and physiological hydrogen carbonate buffer from polymer blend-coated oral solid dosage forms. European Journal of Pharmaceutical Sciences 77:246-253.
6. Sakamoto A, Izutsu K, Yoshida H, Abe Y, Inoue D, Sugano K 2021. Simple bicarbonate buffer system for dissolution testing: Floating lid method and its application to colonic drug delivery system. Journal of Drug Delivery Science and Technology 63.
7. Shibata H, Yoshida H, Izutsu KI, Goda Y 2016. Use of bicarbonate buffer systems for dissolution characterization of enteric-coated proton pump inhibitor tablets. Journal of Pharmacy and Pharmacology 68(4):467-474.
8. Liu F, Merchant HA, Kulkarni RP, Alkademi M, Basit AW 2011. Evolution of a physiological pH 6.8 bicarbonate buffer system: Application to the dissolution testing of enteric coated products. European Journal of Pharmaceutics and Biopharmaceutics 78(1):151-157.
9. Varum FJO, Merchant HA, Goyanes A, Aasi P, Zboranova V, Basit AW 2014. Accelerating the dissolution of enteric coatings in the upper small intestine: Evolution of a novel pH 5.6 bicarbonate buffer system to assess drug release. International Journal of Pharmaceutics 468(1-2):172-177.

10. McNamara DP, Whitney KM, Goss SL 2003. Use of a physiologic bicarbonate buffer system for dissolution characterization of ionizable drugs. Pharmaceutical Research 20(10):1641-1646.
11. Sheng JJ, McNanara DP, Amidon GL 2009. Toward an In Vivo Dissolution Methodology: A Comparison of Phosphate and Bicarbonate Buffers. Molecular Pharmaceutics 6(1):29-39.
12. Krieg BJ, Taghavi SM, Amidon GL, Amidon GE 2015. In Vivo Predictive Dissolution: Comparing the Effect of Bicarbonate and Phosphate Buffer on the Dissolution of Weak Acids and Weak Bases. Journal of Pharmaceutical Sciences 104(9):2894-2904.
13. Al-Gousous J, Salehi N, Amidon GE, Ziff RM, Langguth P, Amidon GL 2019. Mass Transport Analysis of Bicarbonate Buffer: Effect of the CO2-H2CO3 Hydration-Dehydration Kinetics in the Fluid Boundary Layer and the Apparent Effective pK(a) Controlling Dissolution of Acids and Bases. Molecular Pharmaceutics 16(6):2626-2635.
14. Jede C, Wagner C, Kubas H, Weigandt M, Weber C, Lecomte M, Badolo L, Koziolek M, Weitschies W 2019. Improved Prediction of in Vivo Supersaturation and Precipitation of Poorly Soluble Weakly Basic Drugs Using a Biorelevant Bicarbonate Buffer in a Gastrointestinal Transfer Model. Molecular Pharmaceutics 16(9):3938-3947.
15. Kostewicz ES, Wunderlich M, Brauns U, Becker R, Bock T, Dressman JB 2004. Predicting the precipitation of poorly soluble weak bases upon entry in the small intestine. Journal of Pharmacy and Pharmacology 56(1):43-51.
16. O'Dwyer PJ, Litou C, Box KJ, Dressman JB, Kostewicz ES, Kuentz M, Reppas C 2019. In vitro methods to assess drug precipitation in the fasted small intestine - a PEARRL review. Journal of Pharmacy and Pharmacology 71(4):536-556.
17. Brouwers J, Brewster ME, Augustijns P 2009. Supersaturating Drug Delivery Systems: The Answer to Solubility-Limited Oral Bioavailability? Journal of Pharmaceutical Sciences 98(8):2549-2572.
18. Taylor LS, Zhang GGZ 2016. Physical chemistry of supersaturated solutions and implications for oral absorption. Advanced Drug Delivery Reviews 101:122-142.
19. Kuentz M 2019. Drug supersaturation during formulation digestion, including real-time analytical approaches. Advanced Drug Delivery Reviews 142:50-61.
20. Krollik K, Lehmann A, Wagner C, Kaidas J, Kubas H, Weitschies W 2022. The effect of buffer species on biorelevant dissolution and precipitation assays-Comparison of phosphate and bicarbonate buffer. European Journal of Pharmaceutics and Biopharmaceutics 171:90-101.
21. Galia E, Nicolaides E, Horter D, Lobenberg R, Reppas C, Dressman JB 1998. Evaluation of various dissolution media for predicting in vivo performance of class I and II drugs. Pharmaceutical Research 15(5):698-705.
22. Vertzoni M, Dressman J, Butler J, Hempenstall J, Reppas C 2005. Simulation of fasting gastric conditions and its importance for the in vivo dissolution of lipophilic compounds. European Journal of Pharmaceutics and Biopharmaceutics 60(3):413-417.
23. Markopoulos C, Andreas CJ, Vertzoni M, Dressman J, Reppas C 2015. In-vitro simulation of luminal conditions for evaluation of performance of oral drug products: Choosing the appropriate test media. European Journal of Pharmaceutics and Biopharmaceutics 93:173-182.
24. Adler C, Schoenenberger M, Teleki A, Kuentz M 2016. Molecularly designed lipid microdomains for solid dispersions using a polymer/inorganic carrier matrix produced by hot-melt extrusion. International Journal of Pharmaceutics 499(1-2):90-100.
25. Luebbert C, Stoyanov E, Sadowski G 2021. Phase behavior of ASDs based on hydroxypropyl cellulose. International journal of pharmaceutics: X 3:100070-100070.
26. Bachmaier RD, Monschke M, Faber T, Krome AK, Pellequer Y, Stoyanov E, Lamprecht A, Wagner KG 2021. In vitro and in vivo assessment of hydroxypropyl cellulose as functional additive for enabling formulations containing itraconazole. International journal of pharmaceutics: X 3:100076-100076.

27. Niederquell A, Stoyanov E, Kuentz M 2022. Hydroxypropyl Cellulose for Drug Precipitation Inhibition: From the Potential of Molecular Interactions to Performance Considering Microrheology. Molecular Pharmaceutics 19(2):690-703.
28. Guzman HR, Tawa M, Zhang Z, Ratanabanangkoon P, Shaw P, Gardner CR, Chen H, Moreau J-P, Almarsson O, Remenar JF 2007. Combined use of crystalline salt forms and precipitation inhibitors to improve oral absorption of celecoxib from solid oral formulations. Journal of Pharmaceutical Sciences 96(10):2686-2702.
29. Misic Z, Jung D, Sydow G, Kuentz M 2014. Understanding the interactions of oleic acid with basic drugs in solid lipids on different biopharmaceutical levels. Journal of Excipients and Food Chem 5(2):113-134.
30. Krieger E, Vriend G 2014. YASARA View-molecular graphics for all devices-from smartphones to workstations. Bioinformatics 30(20):2981-2982.
31. Krieger E, Dunbrack RL, Jr., Hooft RWW, Krieger B 2012. Assignment of protonation states in proteins and ligands: combining pKa prediction with hydrogen bonding network optimization. Methods in molecular biology (Clifton, NJ) 819:405-421.
32. Krieger E, Vriend G 2015. New Ways to Boost Molecular Dynamics Simulations. Journal of Computational Chemistry 36(13):996-1007.
33. Kirschner KN, Yongye AB, Tschampel SM, Gonzalez-Outeirino J, Daniels CR, Foley BL, Woods RJ 2008. GLYCAM06: A generalizable Biomolecular force field. Carbohydrates. Journal of Computational Chemistry 29(4):622-655.
34. Wang JM, Wolf RM, Caldwell JW, Kollman PA, Case DA 2004. Development and testing of a general amber force field. Journal of Computational Chemistry 25(9):1157-1174.
35. Jakalian A, Jack DB, Bayly CI 2002. Fast, efficient generation of high-quality atomic charges. AM1-BCC model: II. Parameterization and validation. Journal of Computational Chemistry 23(16):1623-1641.
36. Jorgensen WL, Chandrasekhar J, Madura JD, Impey RW, Klein ML 1983. COMPARISON OF SIMPLE POTENTIAL FUNCTIONS FOR SIMULATING LIQUID WATER. Journal of Chemical Physics 79(2):926-935.
37. Essmann U, Perera L, Berkowitz ML, Darden T, Lee H, Pedersen LG 1995. A SMOOTH PARTICLE MESH EWALD METHOD. Journal of Chemical Physics 103(19):8577-8593.
38. Trott O, Olson AJ 2010. Software News and Update AutoDock Vina: Improving the Speed and Accuracy of Docking with a New Scoring Function, Efficient Optimization, and Multithreading. Journal of Computational Chemistry 31(2):455-461.
39. Schwebel HJ, van Hoogevest P, Leigh MLS, Kuentz M 2011. The apparent solubilizing capacity of simulated intestinal fluids for poorly water-soluble drugs. Pharmaceutical Development and Technology 16(3):278-286.
40. Trandafirescu C, Avram S, Soica C, Aigner Z, Arpad G, Kata M, Dehelean C, Szabadai Z, Borcan F 2014. Solid-state Characterization of Bifonazole - beta-cyclodextrin Binary Systems. II. Revista De Chimie 65(11):1336-1339.
41. Bruning J, Alig E, Schmidt MU 2010. Ezetimibe anhydrate, determined from laboratory powder diffraction data. Acta Crystallographica Section C-Structural Chemistry 66:O341-O344.
42. Sacchi P, Reutzel-Edens SM, Cruz-Cabeza AJ 2021. The unexpected discovery of the ninth polymorph of tolfenamic acid. Crystengcomm 23(20):3636-3647.
43. Tothadi S, Bhogala BR, Gorantla AR, Thakur TS, Jetti RKR, Desiraju GR 2012. Triclabendazole: An Intriguing Case of Co-existence of Conformational and Tautomeric Polymorphism. Chemistry-an Asian Journal 7(2):330-342.
44. Kuentz M, Holm R, Kronseder C, Saal C, Griffin BT 2021. Rational Selection of Bio-Enabling Oral Drug Formulations-A PEARRL Commentary. Journal of Pharmaceutical Sciences 110(5):1921-1930.

45. Alhayali A, Selo MA, Ehrhardt C, Velaga S 2018. Investigation of supersaturation and in vitro permeation of the poorly water soluble drug ezetimibe. European Journal of Pharmaceutical Sciences 117:147-153.
46. Baird JA, Van Eerdenbrugh B, Taylor LS 2010. A Classification System to Assess the Crystallization Tendency of Organic Molecules from Undercooled Melts. Journal of Pharmaceutical Sciences 99(9):3787-3806.
47. Wyttenbach N, Kuentz M 2017. Glass-forming ability of compounds in marketed amorphous drug products. European Journal of Pharmaceutics and Biopharmaceutics 112:204-208.
48. Blaabjerg LI, Lindenberg E, Lobmann K, Grohganz H, Rades T 2018. Is there a correlation between the glass forming ability of a drug and its supersaturation propensity? International Journal of Pharmaceutics 538(1-2):243-249.
49. Blaabjerg LI, Grohganz H, Lindenberg E, Lobmann K, Mullertz A, Rades T 2018. The Influence of Polymers on the Supersaturation Potential of Poor and Good Glass Formers. Pharmaceutics 10(4).
50. Du W, Cruz-Cabeza AJ, Woutersen S, Davey RJ, Yin Q 2015. Can the study of self-assembly in solution lead to a good model for the nucleation pathway? The case of tolfenamic acid. Chemical Science 6(6):3515-3524.
51. Price DJ, Ditzinger F, Kohl NJ, Jankovic S, Tsakiridou G, Nair A, Holm R, Kuentz M, Dressman JB, Saal C 2019. Approaches to increase mechanistic understanding and aid in the selection of precipitation inhibitors for supersaturating formulations - a PEARRL review. Journal of Pharmacy and Pharmacology 71(4):483-509.
52. Desai D, Rinaldi F, Kothari S, Paruchuri S, Li D, Lai M, Fung S, Both D 2006. Effect of hydroxypropyl cellulose (HPC) on dissolution rate of hydrochlorothiazide tablets. International Journal of Pharmaceutics 308(1-2):40-45.
53. Pegram LM, Record MT 2008. Thermodynamic origin of Hofmeister ion effects. Journal of Physical Chemistry B 112(31):9428-9436.
54. Moghaddam SZ, Thormann E 2019. The Hofmeister series: Specific ion effects in aqueous polymer solutions. Journal of Colloid and Interface Science 555:615-635.
55. Kunz W, Lo Nostro P, Ninham BW 2004. The present state of affairs with Hofmeister effects. Current Opinion in Colloid & Interface Science 9(1-2):1-18.
56. Salis A, Ninham BW 2014. Models and mechanisms of Hofmeister effects in electrolyte solutions, and colloid and protein systems revisited. Chemical Society Reviews 43(21):7358-7377.
57. Saal W, Ross A, Wyttenbach N, Alsenz J, Kuentz M 2018. Unexpected Solubility Enhancement of Drug Bases in the Presence of a Dimethylaminoethyl Methacrylate Copolymer. Molecular Pharmaceutics 15(1):186-192.

Figure captions

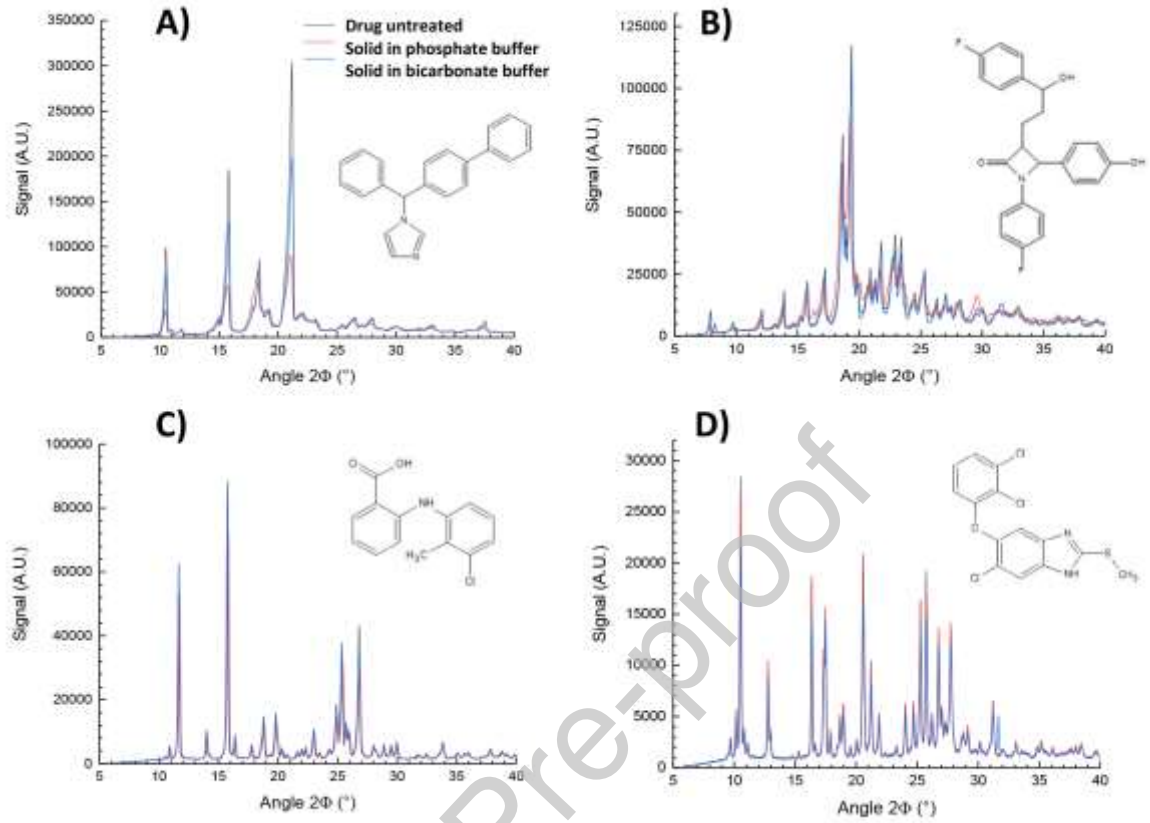

Fig. 1. X-ray powder diffraction (XRPD) patterns as arbitrary units (A.U.) vs. 2 theta (Φ) angle in degrees of A) bifonazole, B) ezetimibe, C) tolfenamic acid, D), triclabendazole. Bragg peaks for untreated drug as reference (gray) and the residual solid of the solubility experiments in phosphate buffer (red) and bicarbonate buffer (blue) are nearly superimposable.

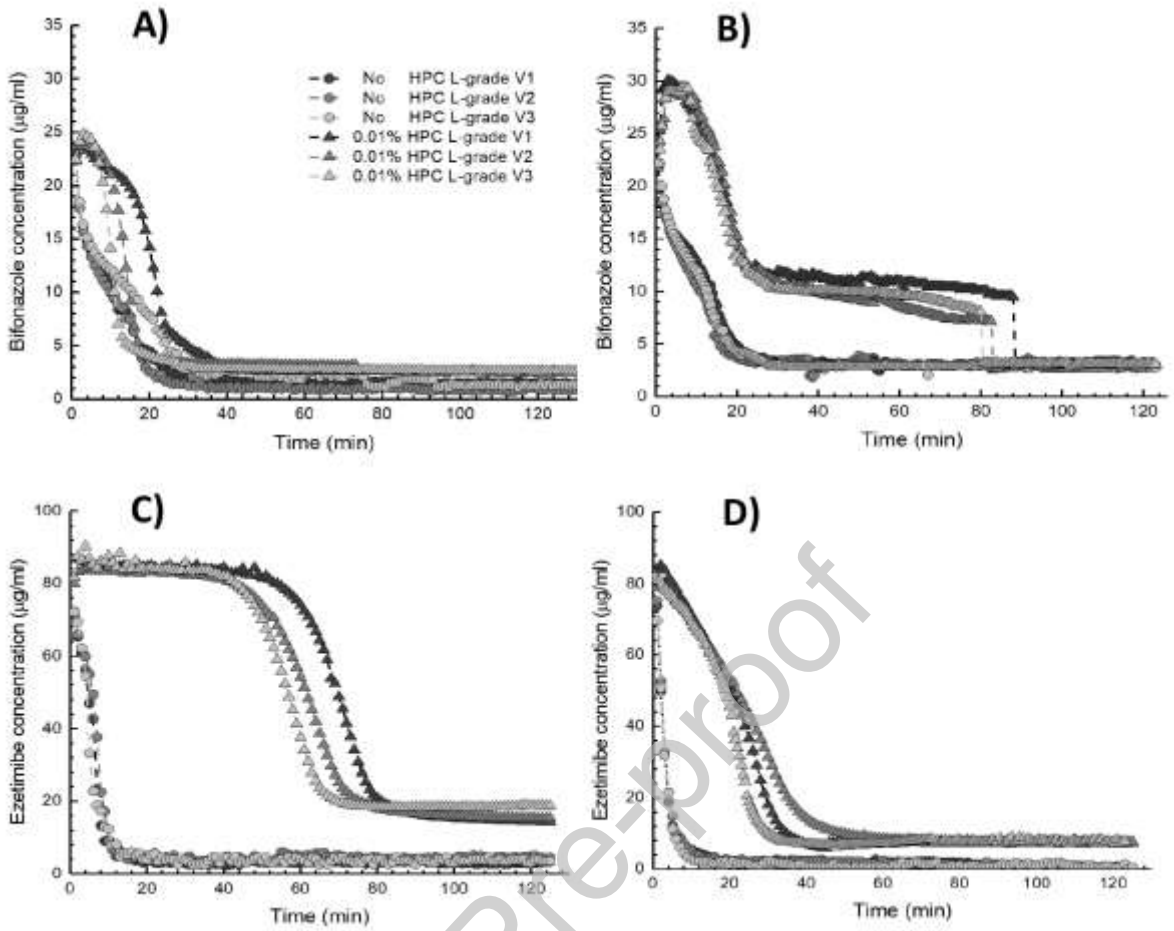

Fig. 2. Desupersaturation kinetics (triplicates, V1-V3) as pure drug solution (circles) and with added 0.01% (w/w) hydroxypropyl cellulose (HPC) L-grade (triangles) at pH 6.5 and 37°C for A) bifonazole (phosphate buffer), B) bifonazole (bicarbonate buffer), C) ezetimibe (phosphate buffer), D) ezetimibe (bicarbonate buffer).

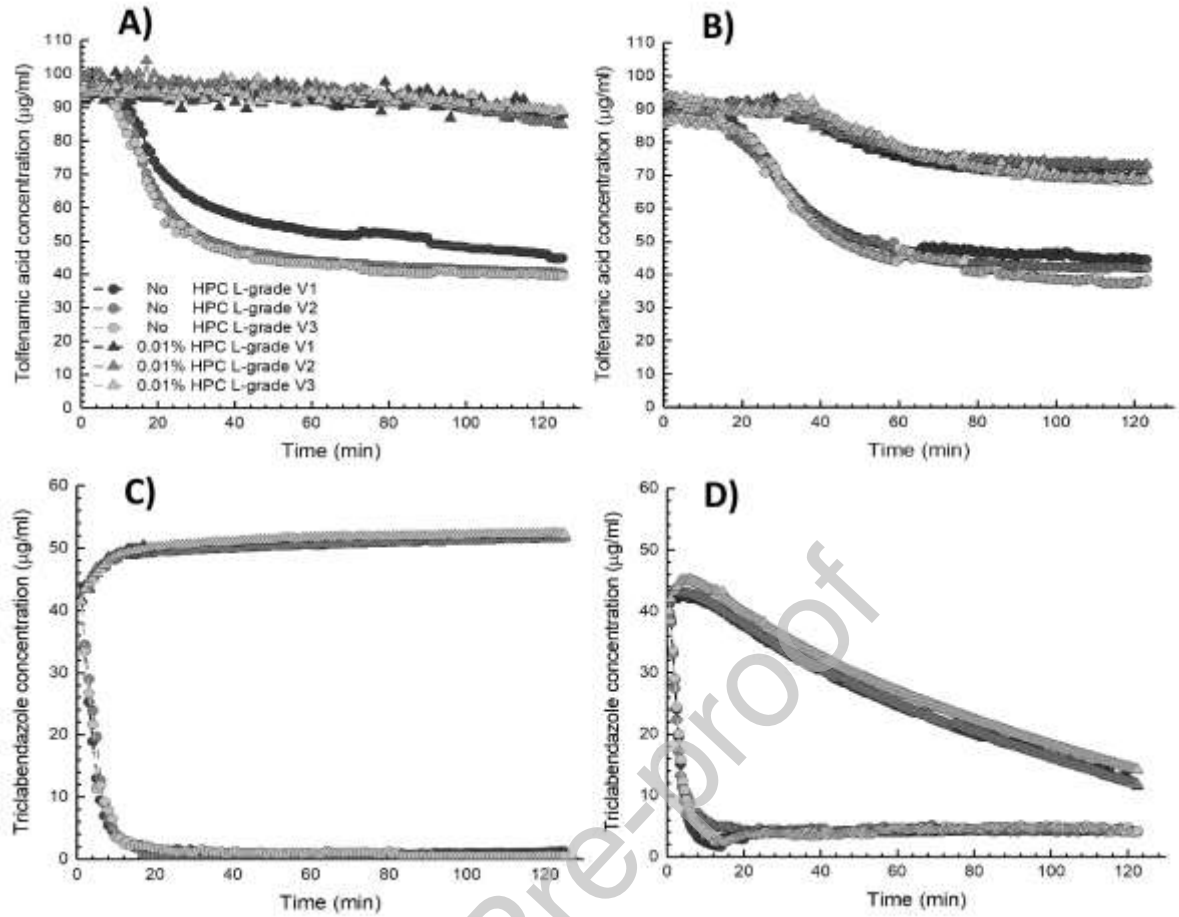

Fig. 3. Desupersaturation kinetics (triplicates, V1-V3) as pure drug solution (circles) and with added 0.01% (w/w) HPC L-grade (triangles) at pH 6.5 and 37°C for A) tolfenamic acid (phosphate buffer), B) tolfenamic acid (bicarbonate buffer), C) triclabendazole (phosphate buffer), D) triclabendazole (bicarbonate buffer).

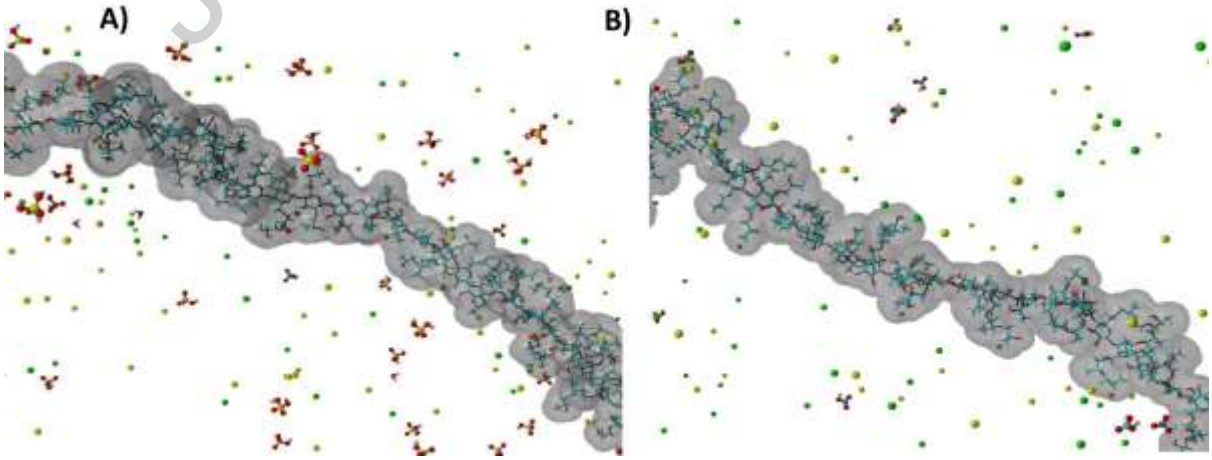

Fig. 4. Results of a molecular dynamics (MD) simulation (n= 40 oligomer, 5 ns, periodic boundary conditions, 37°C, pH 6.5) comparing the solvent accessible surface area of HPC in A) phosphate and B) bicarbonate buffer. Ions are shown as ball and stick model, while water is not visible for clarity of presentation. Details are given in the text.

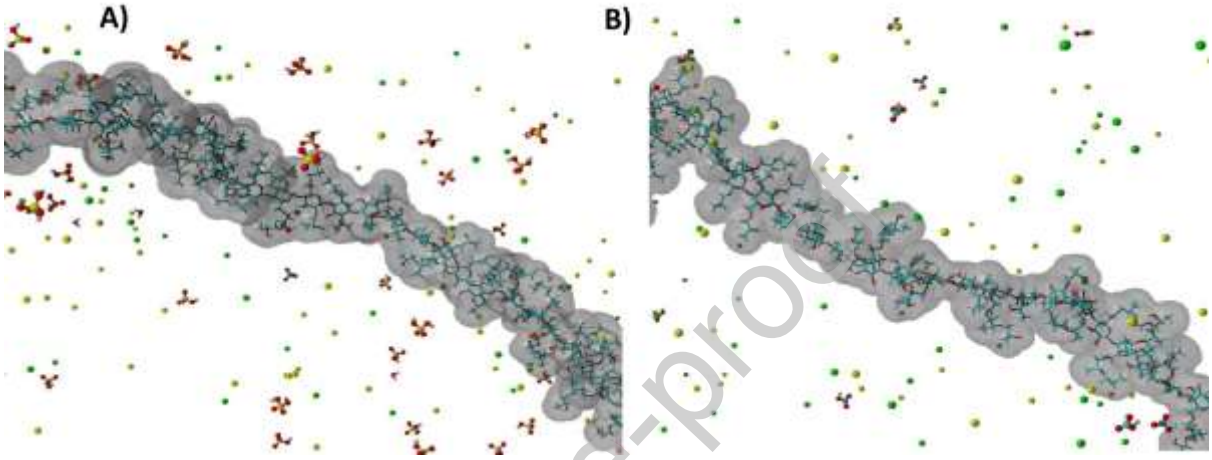

Fig. 5. Interaction plot of two-way analysis of the variance (ANOVA) based on drug-HPC interaction energies obtained from molecular docking simulations. Phosphate buffer results are given as black circles (solid line), whereas blue triangles (dashed line) represent corresponding drug-HPC interaction energies for bicarbonate buffer. Details are given in the text.

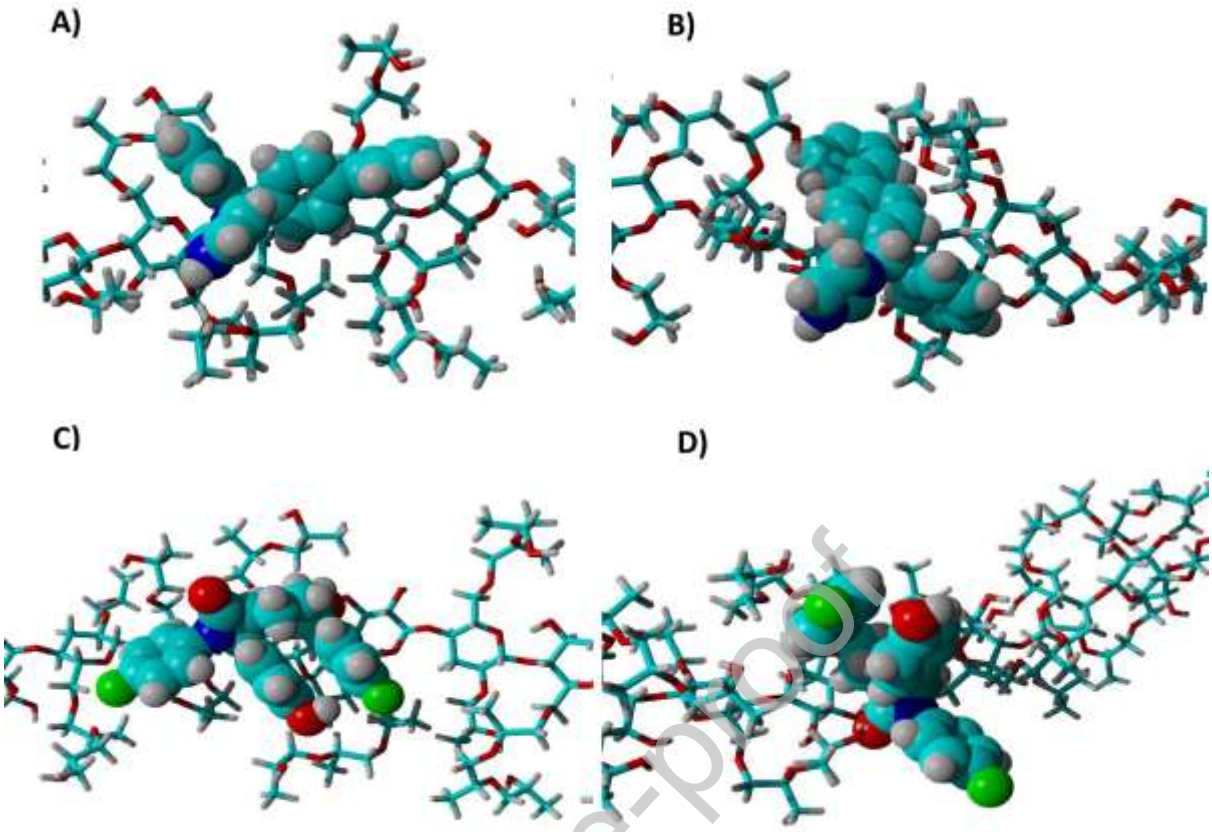

Fig. 6. Molecular docking of HPC with model compounds. Lowest-energy binding conformation is depicted for A) bifonazole (phosphate buffer) B) bifonazole (bicarbonate buffer), C) ezetimibe (phosphate buffer), D) ezetimibe (bicarbonate buffer).

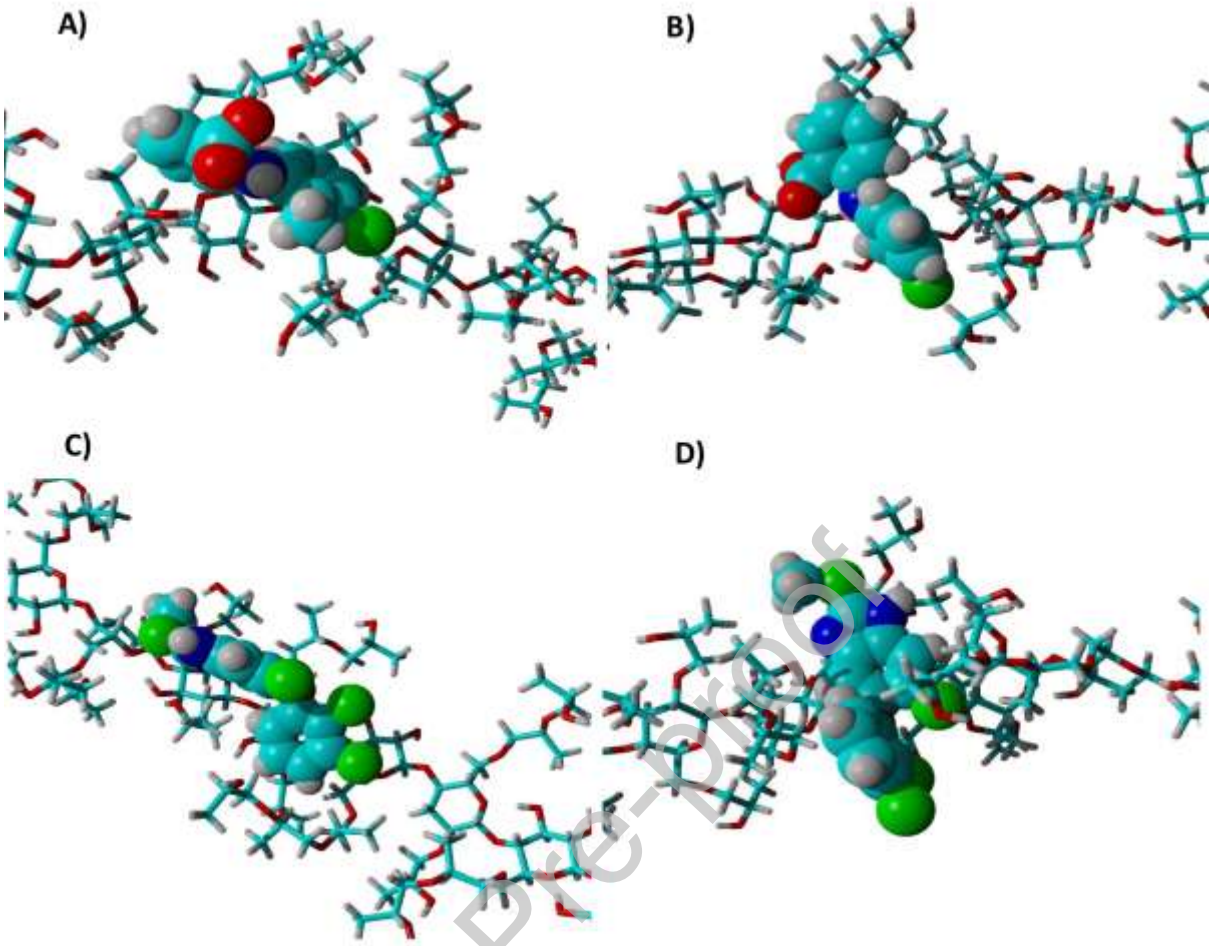

Fig. 7. Molecular docking of HPC with model compounds. Lowest-energy binding conformation is depicted for A) tolfenamic acid (phosphate buffer) B) tolfenamic acid (bicarbonate buffer), C) triclabendazole (phosphate buffer), D) triclabendazole (bicarbonate buffer).

Tables

Table 1 – Composition of buffers used (pH 6.5)

	Phosphate buffer	Bicarbonate buffer
NaCl (mM)	77.5	111.8
NaH_2PO_4 (mM)	56.8	
NaOH (mM)	q.s. pH 6.5	
$NaHCO_3$ (mM)		22.5
CO_2 (mM)		q.s. pH 6.5
Buffer capacity (mmol/L /ΔpH)	~20	

Table 2 – Drug solubility results

	Solubility in phosphate buffer (μg/mL)	Solubility in bicarbonate buffer (μg/mL)
Bifonazole	0.58 ± 0.01	0.16 ± 0.01
Ezetimibe	0.14 ± 0.00	0.23 ± 0.02
Tolfenamic acid	26.21 ± 0.34	39.72 ± 0.24
Triclabendazole	0.49 ± 0.01	3.96 ± 0.02

Table 3 – Induction times of drug precipitation as means with standard deviations (n=3)

	Induction time in phosphate buffer (min)	Induction time in bicarbonate buffer (min)
Bifonazole	0	0
Bifonazole with 0.01% (w/w) HPC	7.3 ± 0.6	14.2 ± 0.8
Ezetimibe	0	0
Ezetimibe with 0.01% (w/w) HPC	45.0 ± 6.1	2.7 ± 1.2
Tolfenamic acid	8.0 ± 1.7	15.7 ± 1.6
Tolfenamic acid with 0.01% (w/w) HPC	> 120	32.8 ± 4.5
Triclabendazole	0	0
Triclabendazole with 0.01% (w/w) HPC	> 120	17.8 ± 2.8

Table 4 – MD simulation results of n= 40 HPC oligomer in phosphate vs. bicarbonate buffer. Solvent accessible surface area (SASA) was estimated in snapshot simulations at 310 K (1 bar) after 5 ns of three independent simulation runs. The respective *p*-values for the time and buffer effect are also listed (two- factor ANOVA).

MD simulations n= 40 HPC oligomer	Phosphate buffer	Bicarbonate buffer
SASA at 5 ns	12600 ± 312 Å^2	13233 ± 302 Å^2
Change compared to initial value	-12%	-8%
p-value of time effect	< 0.0001	
p- value of buffer effect	0.0381	